Experimental and theoretical investigation of the electronic structure of transition metal sulphides: CuS, FeS_2 and $FeCuS_2$

Experimental and theoretical investigation of the electronic structure of transition metal sulphides: CuS, FeS$_2$ and FeCuS$_2$

E Z Kurmaev†‡, J van Ek‡, D L Ederer‡, L Zhou§, T A Callcott§,
R C C Perera‖, V M Cherkashenko†, S N Shamin†, V A Trofimova†,
S Bartkowski¶, M Neumann¶, A Fujimori$^+$ and V P Moloshag*

† Institute of Metal Physics, Russian Academy of Sciences—Ural Division, 620219
Yekaterinburg, GSP-170, Russia
‡ Department of Physics, Tulane University, New Orleans, LA 70118, USA
§ Department of Physics, University of Tennessee, Knoxville, TN 37996, USA
‖ Lawrence Berkeley Laboratory, Berkeley, CA 94720, USA
¶ Universität Osnabrück, Fachbereich Physik, D-49069 Osnabrück, Germany
$^+$ Department of Physics, University of Tokyo, Hongo, Bunkyo-Ku, Tokyo 113, Japan
* Institute of Geology and Geochemistry, Russian Academy of Sciences—Ural Division,
620151 Yekaterinburg, Russia

Abstract.   Results of measurements of sulphur L$_{2,3}$ x-ray emission spectra of CuS and FeS$_2$, excited by synchrotron radiation near the sulphur 2p threshold, are presented. An excitation energy dependence of the sulphur L$_{2,3}$ XES is only observed for CuS, and is attributed to the presence of inequivalent sulphur atoms in CuS. Two thirds of the sulphur atoms form S$_2$ dimers (as in FeS$_2$) while the remaining ones are single (as in CuFeS$_2$). This conclusion is confirmed by XPS measurements and LMTO band structure calculations for CuS, FeS$_2$ and CuFeS$_2$. It is shown that selective excitation of x-ray emission valence spectra can be used to determine the atom-decomposed partial density of states for inequivalent sites in solids, occupied by chemically identical species.

1. Introduction

Recent developments in instrumentation and synchrotron radiation sources give a new impulse to the study of the electronic structure of solids with the aid of soft-x-ray emission spectroscopy (XES) [1, 2]. As a result of the high brightness of third-generation synchrotron sources, the intensity of fluorescence x-ray emission in the soft-x-ray energy range (where non-radiative decay processes of core vacancy states is dominant [3]) has increased. This makes it possible to study the electronic structure of impurity atoms in different materials [4, 5]. Use of tunable synchrotron radiation for excitation of XES has several advantages for the study of the electronic structure. First, selective excitation of XES avoids the overlap of satellites and valence spectra that originate from transitions into the spin–orbit split core levels (L$_{2,3}$, M$_{2,3}$, M$_{4,5}$ etc). This is important for the analysis of the density of states (DOS) in the vicinity of the Fermi level in 3d, 4d and 5d transition metal alloys and compounds [6]. Second, chemically identical atoms at inequivalent sites in the crystal can be

♯ Corresponding author. E-mail address: kurmaev@ifmlrs.uran.ru

subsequently excited as the excitation energy increases. Hence, the local electronic structure of atoms with electrons in states at slightly different binding energies can be determined [7–9].

The present paper describes how tunable synchrotron radiation was used for selective excitation of inequivalent sulphur atoms in CuS. Thus, for the first time, the sulphur $L_{2,3}$ XES of S_I atoms that form S_2 dimers is measured separately. The obtained results compare favourably with the density of states obtained from density functional band structure calculations.

2. Experimental and computational details

High-energy resolved S $L_{2,3}$ x-ray emission spectra (valence 3s3d $\rightarrow$ 2p transition) of CuS and FeS_2 were measured at the Advanced Light Source (ALS) Beamline 8.0, a 5.0 cm period undulator beamline with a spherical grating monochromator operating between 70 eV and 1200 eV. The energy resolution of the monochromator was set to about 0.3 eV during these measurements. The soft-x-ray endstation includes a Rowland circle grating spectrometer coupled to a photon-counting area detector [10]. All soft-x-ray emission spectra reported in this work were recorded with a 100 μm entrance slit for the spectrometer that had a 1500 lines mm^{-1}, 10 m radius grating as the dispersing element. Photon energies range from 161.5 to 169.5 eV. The energy resolution is estimated to be 0.15 eV at 150 eV, and the spectra were taken under high vacuum (10^{-9} mbar).

S $L_{2,3}$ x-ray emission spectra (valence 3s3d $\rightarrow$ 2p transition) of $CuFeS_2$ were measured with an ultrasoft-x-ray spectrometer [11] with high spatial ($\Delta S = 4$–5 μm) and energy ($\Delta E = 0.4$ eV) resolution using electron excitation. For analysis of the x-ray radiation, a diffraction grating was used ($N = 600$ lines mm^{-1}; $R = 2$ m). The accelerating voltage on the x-ray tube was 4 keV and the anode current was 130 nA.

The Fe Lα and Cu Lα (valence 3d4s $\rightarrow$ 2p$_{3/2}$ transition) x-ray emission spectra were generated by means of electron excitation and measured on a RSM-500-type x-ray vacuum spectrometer with a diffraction grating ($N = 600$ lines mm^{-1} and $R = 6$ m). The spectra were recorded in the second order of reflection by a secondary-electron multiplier with a CsI photocathode. For Fe Lα and Cu Lα the energy resolutions were 0.35 and 0.40 eV, respectively. The x-ray tube was operated at $V = 4$ keV and $I = 0.4$ mA.

The S $K\beta_1$ (valence 3p $\rightarrow$ 1s transition) x-ray emission spectrum was measured using a fluorescent Johan-type vacuum spectrometer with a position-sensitive detector [12]. Pd L x-ray radiation from a sealed x-ray tube was used for the excitation of the fluorescent S $K\beta_1$ spectra. A quartz(1010) single crystal curved to $R = 1400$ mm served to disperse the radiation. The spectra were measured with an energy resolution of approximately 0.25 eV. The x-ray tube was operated at $V = 25$ keV and $I = 50$ mA.

The XPS measurements of CuS, FeS_2 and $CuFeS_2$ were performed with an ESCA spectrometer from Physical Electronics (PHI 5600 ci, with monochromatized Al Kα radiation of 0.3 eV FWHM). The energy resolution of the analyser was 1.5% of the pass energy. The estimated energy resolution was less than 0.35 eV for the XPS measurements on the copper and iron sulphides. The pressure in the vacuum chamber during the measurements was below 5×10^{-9} mbar. All of the investigated compounds were available as single crystals. Prior to XPS measurements the crystals were cleaved in ultra-high vacuum. All the investigations have been performed at room temperature on the freshly cleaved surface. Thus, excellent surfaces, with minimal concentrations of defects and contaminations, were obtained. As a result the intrinsic properties of the samples could be studied. The XPS spectra were calibrated using a Au foil to obtain photoelectrons from the Au 4f$_{7/2}$ subshell.

The binding energy for Au $4f_{7/2}$ electrons is 84.0 eV.

Electronic structure calculations for CuS, FeS_2 and $CuFeS_2$ were performed with the linear muffin-tin orbital method in the atomic sphere approximation (LMTO–ASA) [13]. Exchange and correlation effects are treated within the local density approximation (LDA) of density functional theory [14]. Self-consistent solutions of the Kohn–Sham equations are obtained for all electrons in the system using the exchange–correlation potential as parametrized by von Barth and Hedin [15].

The crystal structure of CuS, or covellite, is hexagonal (space group 194, $P63/mmc$). According to Wyckoff [16] $a = 3.796$ Å and $c = 16.36$ Å and the unit cell contains six formula units with two inequivalent sites for both Cu and S. Two thirds of the sulphur atoms in CuS form dimers, while the remaining S atoms are single. Pyrite, or FeS_2, forms a cubic crystal with $a = 5.406\,67$ Å [16] (space group 205, $Pa3$). All the sulphur atoms in FeS_2 form dimers. Chalcopyrite, or $CuFeS_2$, is an antiferromagnetic insulator with a body-centred tetragonal unit cell (space group 82, $I4$). Lattice constants according to Wyckoff [16] are $a = 5.24$ Å and $c = 10.30$ Å. Empty spheres were added at the Wyckoff position (8d). All the sulphur atoms in $CuFeS_2$ are single. Previously reported results on the band structure of $CuFeS_2$ [17] are in agreement with results obtained in the present work.

Whereas the basis set for the transition metal atoms includes s-, p- and d-type functions, only s and p functions were included for sulphur. Pivotal energies are chosen at the centre of gravity of the occupied, atom decomposed partial density of states. All atomic spheres for a given crystal have the same radius. For each system the irreducible wedge was sampled with approximately 250 k-points in a linear tetrahedron method.

3. Results and discussion

In figure 1(a) the S $L_{2,3}$ XES of CuS measured at different excitation energies (from 161.5 to 169.5 eV) are shown. The spectra are normalized to the total number of incident photons which is calculated from the product of the incident x-ray flux and the exposure time. An excitation energy dependence of the S $L_{2,3}$ XES is found for CuS, whereas similar measurements for S $L_{2,3}$ XES of FeS_2 show an unchanged shape of the emission band at different excitation energies (figure 1(b)). The fluorescence S $L_{2,3}$ XES spectra of CuS excited at photon energies $E = 162.5$ eV and $E = 163.5$ eV are found to be rather different. The spectrum excited at $E = 162.5$ eV is narrower than the one at $E = 163.5$ eV, and its intensity maximum is shifted 2 eV toward lower photon energy.

For the analysis of the obtained results we first consider the XPS S 2p spectra of CuS and reference compounds FeS_2 and $CuFeS_2$ shown in figure 2 as diamonds. The intensity ratio of the S $2p_{1/2}$ and S $2p_{3/2}$ lines is close to 1:2 for FeS_2 and $CuFeS_2$ but significantly deviates from this ratio for CuS (0.82:1). Moreover, an additional high-energy shoulder has appeared in the S 2p spectra of CuS at 163.8 eV. A glance at the XPS spectra for the reference compounds show that the binding energy for S 2p electrons for S_2 dimers and single sulphur atoms can be quite different. It is therefore reasonable to assume that the CuS XPS spectrum is a superposition of single sulphur atoms and S_2 dimers with ratio 1:2. Hence, the XPS spectrum reflects the inequivalent environment of the two types of sulphur atom in the CuS crystal [18]. From LMTO calculations the energy for the 2p levels in CuS was found to be different for S_I and S_{II}. The spin–orbit splitting between $S_{II}\,2p_{1/2}$ and $S_{II}\,2p_{3/2}$ is 1.24 eV. The $S_I\,2p_{1/2}$ state of the $S_I\,2p_{1/2}$–$2p_{3/2}$ doublet with the same spin–orbit splitting is placed 0.68 eV lower in binding energy, above $S_{II}\,2p_{3/2}$. Here S_I are in dimers and S_{II} are the single sulphur atoms. Assuming the $S_{II}\,2p_{3/2}$ and $S_I\,2p_{1/2}$ at equal energy one deduces a peak ratio of 1:4:4. However, an energy difference between
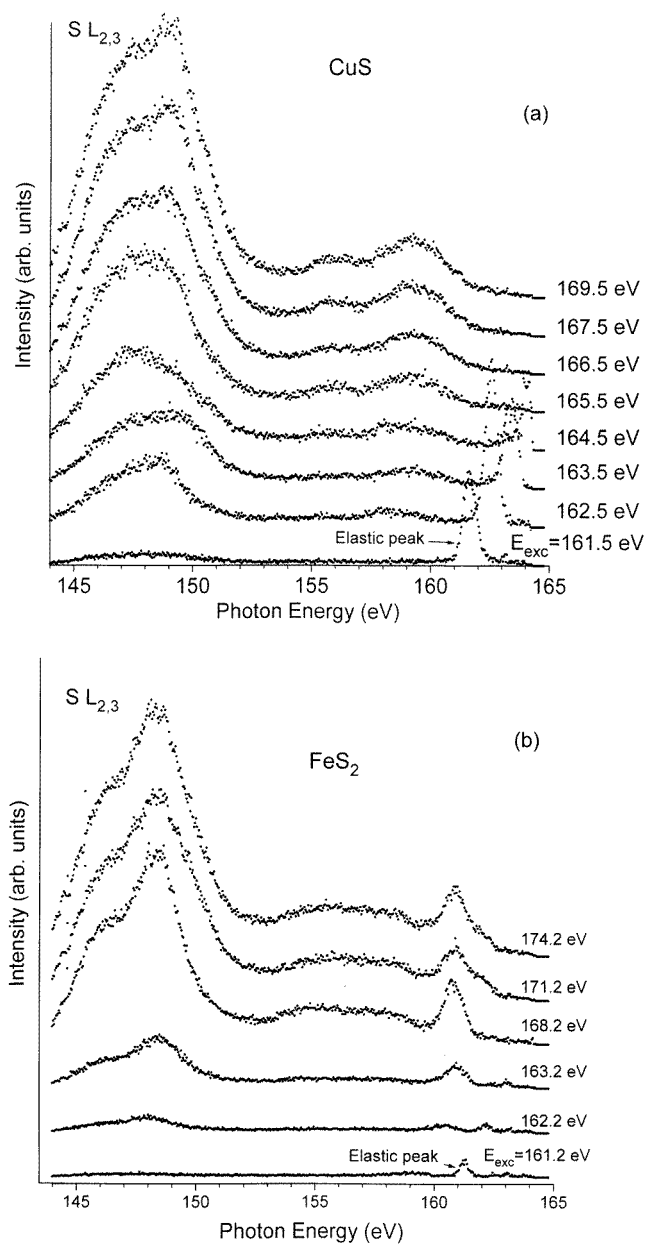
Figure 1. S $L_{2,3}$ XES of CuS (a) and FeS_2 (b) measured at different excitation energies.

these core levels broadens the central peak and reduces its intensity. A simulation of the superposition of the two 2p spectra (dashed curve and thin solid curve in figure 2) is shown at the thick solid curve in figure 2. Reasonable agreement with experiment is obtained if two typical S 2p spectra are shifted by 1.6 eV and are superimposed with ratio 1:2. The spectrum at lower binding energy corresponds to sulphur dimers. The spin–orbit splitting deduced from the 2p XPS spectra for $CuFeS_2$ or FeS_2 is about 1.15 eV, slightly less than
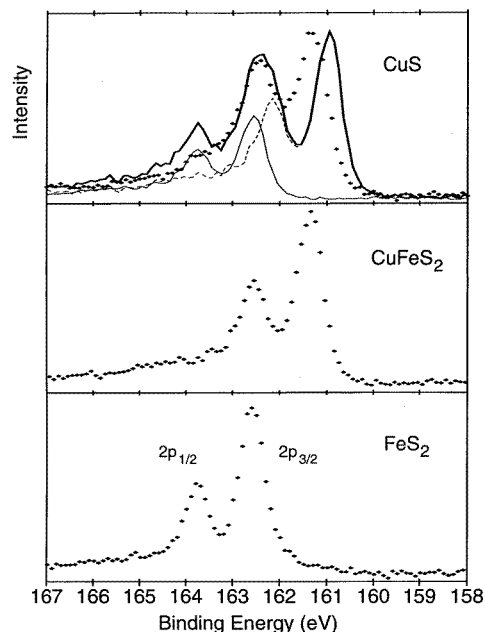
Figure 2. XPS S 2p of CuS, FeS$_2$ and CuFeS$_2$ (diamonds). The solid and dashed lines indicate the simulated XPS of CuS (see text).

the theoretical value. Combining the experimental spin–orbit splitting with the 1.6 eV shift leads to a S$_{II}$ 2p$_{3/2}$ versus S$_I$ 2p$_{1/2}$ splitting of 0.55 eV, in fair agreement with the theoretical result (0.68 eV).

Direct superposition of the experimental XPS spectra in figure 2 for CuFeS$_2$ (single S atoms) and FeS$_2$ (S$_2$ dimers), with the correct weight, does not represent the CuS (both single and dimers) spectrum very well. The ratio of peak heights is not reproduced at all, although the peak positions are about right. It is not surprising that this simple superposition argument does not apply to CuS. The crystal structures of the three compounds are very different. Therefore the electrostatic Madelung contribution to the effective potential in which the 2p electrons move will be different. The fact that the XPS peak positions for CuFeS$_2$ and FeS$_2$ are similar to those in CuS is fortuitous.

Application of these findings to the interpretation of the fluorescence spectra leads to the conclusion that at $E = 162.5$ eV only S$_I$ atoms are excited, and at $E = 163.5$ eV both S$_I$ and S$_{II}$ atoms are excited. According to the dipole selection rule, S L$_{2,3}$ XES corresponds to s $\rightarrow$ p and d $\rightarrow$ p transitions that probe S 3s(3d) states in the valence band. Resonant excitation of S$_I$ L$_{2,3}$ and S$_{II}$ L$_{2,3}$ XES imposes an additional constraint. Thus, S L$_{2,3}$ XES excited at $E = 162.5$ eV probe the S$_I$ 3s(3d) DOS and excitation with $E = 163.5$ eV gives information about the combined S$_I$ + S$_{II}$ 3s(3d) DOS of CuS as shown in figure 3(a) where the appropriate data are plotted on a binding energy scale. For FeS$_2$ S L$_{2,3}$, XES at different excitation energies† simply probes the single-sulphur 3s(3d) DOS as shown in figure 3(b). To verify this conclusion LMTO electronic structure calculations were performed for CuS and the two reference compounds, FeS$_2$ and CuFeS$_2$. The results are shown in figures 4–6. A single S 3s band, located 14 eV below the Fermi level, is calculated for CuFeS$_2$ (figure 4),

---

† In figure 3 the S L$_{2,3}$ of CuS and FeS$_2$ are adjusted to the binding energy scale using XPS data in figure 2.

while two 3s-derived subbands form for FeS_2 (figure 5). This splitting is due to the $\sigma-\sigma^*$ energy separation of S-3s-derived molecular orbitals in S_2 dimers in the FeS_2 crystal. For CuS three peaks in the S 3s DOS are seen (figure 6). This structure can be viewed as a superposition of S 3s bands of FeS_2 and $CuFeS_2$ because in CuS there are two different types of S atom: single S atoms as in $CuFeS_2$ and S_2 dimers as in FeS_2. The theoretical contribution of S_I and S_{II} to the DOS of CuS is shown in figure 6. The S_{II} 3s band is narrower than the S_I 3s band, which is split into σ and σ^* subbands. These results support the present interpretation of the S $L_{2,3}$ XES for CuS at different excitation energies shown in figure 1.

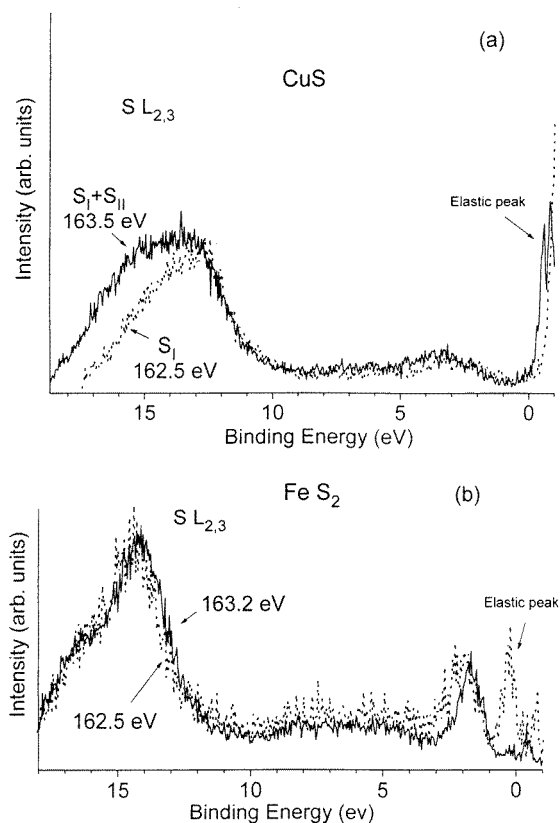**Figure 3.** S $L_{2,3}$ XES of (a) CuS and (b) FeS_2 at the S 2p threshold, with binding energies on the horizontal axis.

In figure 7 the XES (Fe $L\alpha$, S $L_{2,3}$ and S $K\beta_1$) and valence band XPS (XPS VB) of FeS_2 are presented versus the binding energy. These data support the results of band structure calculations shown in figure 5. The energy position of Fe $L\alpha$ XES coincides with the sharp peak in the XPS VB and confirms that it has 3d character. The S $K\beta_1$ spectrum shows the location of the S 3p band. The distinct high-binding-energy shoulder on the Fe $L\alpha$ XES found in this region shows strong admixture of Fe 3d states in the S-3p-like band. S $L_{2,3}$ XES reflects that the low-energy feature of XPS VB must correspond to the S 3s partial DOS. Additional information about the S 3p/Fe 3d hybridization can be obtained from the comparison of XES and XPS VB of FeS_2. Both S $K\beta_1$ and S $L_{2,3}$ XES extend
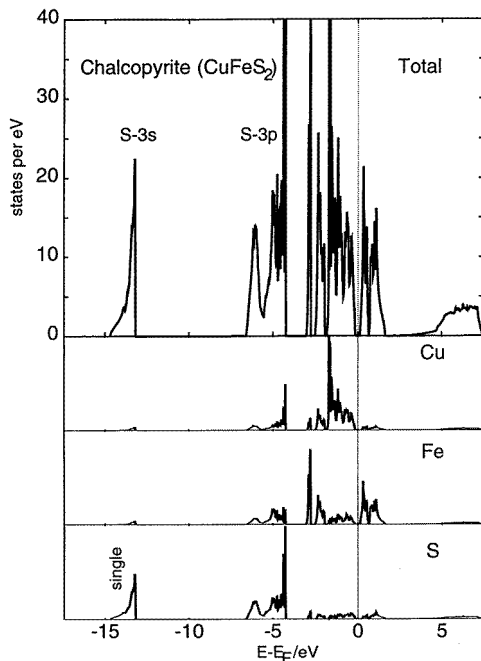
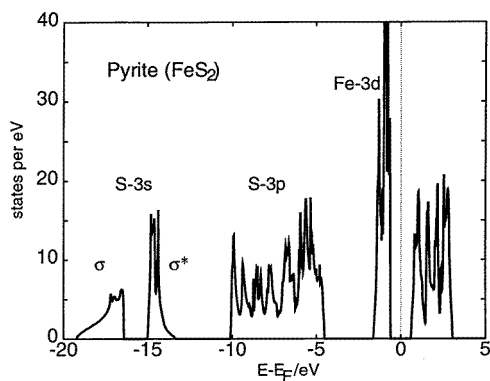**Figure 4.** Calculated total and atom-decomposed DOS of $CuFeS_2$.

Figure 5. Calculated total and atom-decomposed DOS of FeS_2.

to low binding energies, close to the 3d peaks of Fe Lα XES and XPS VB. The feature in S L$_{2,3}$ XES around 2 eV binding energy can be attributed to S 3d density of states because according to results of band structure calculations of FeS_2 given in figure 4 S 3s states are absent in this energy region. According to dipole selection rules S 3d $\to$ 2p transitions are allowed under excitation of S L$_{2,3}$ XES and S 3d states can be directly revealed in these spectra. This means that S 3d orbitals take part in chemical bonding in 3d transition metal sulphides. The problem of participation of 3d atomic orbitals (AOs) of second-row elements (Al, Si, P, S, Cl) in chemical bonding has been discussed in the literature for more than 25 years (see [20]) because the spatial sizes of 3d orbitals of neutral atoms of these
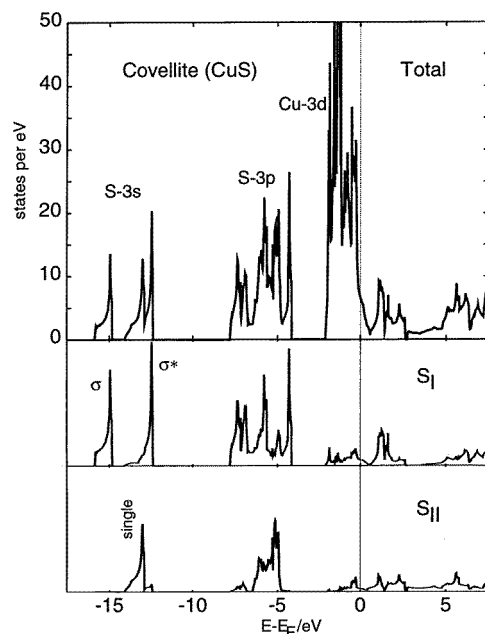
Figure 6. Calculated total and atom-decomposed DOS of CuS.

elements are four to five times higher than those of 3s and 3p orbitals which can prevent participation of 3d AOs in chemical bonding for most chemical compounds. However, as shown in [21], the spatial sizes of S 3d AOs can be reduced to those of S 3s and S 3p AOs under formation of positive charge on the S atom in $LiSO_4$, $(NH_4)_2SO_4$ and SF_6 and their experimental x-ray emission spectra can be explained only under supposition of participation of S 3d AOs in chemical bonding. The special MO LCAO quantum chemistry calculations (see the references in [21]) confirmed this supposition. On the other hand, it was shown that Si 3d AOs take part in chemical bonding in c-SiO_2 [22] and transition metal silicides [11, 23–25], i.e. independently of formal positive or negative charge of Si atoms in compounds.

Combined results of XES (Cu Lα, Fe Lα, S $L_{2,3}$ and S $K\beta_1$) and XPS VB of $CuFeS_2$ are shown in figure 8. The intensity maximum of Cu Lα XES is at the same binding energy as for Fe Lα XES, and is located near the main maximum of XPS VB, and provides evidence for a strong Cu 3d/Fe 3d hybridization. Both maxima are very close to the shoulder of S $K\beta_1$ XES and one concludes that Fe 3d/S 3p and Cu 3d/S 3p mixing takes place. Fe Lα XES extends to higher binding energy then Cu Lα, again suggesting that there is significant Fe 3d/S 3p hybridization in the valence band, in accordance with results from band structure calculations (figure 4). Our results do not reproduce the two-peak character of the Fe 3d DOS obtained in [19] by subtracting XPS of $CuFeS_2$ and $CuAl_{0.9}Fe_{0.1}S_2$.

The more complicated fine structure of the S 3s band of FeS_2, due to σ–σ^* separation of S 3s states in S_2 dimers as obtained in the band structure calculations, can be seen in XPS VB of FeS_2 shown in figure 7. In the XPS spectra and the computed DOS for $CuFeS_2$ a splitting of the S 3s band is not observed. The S $L_{2,3}$ XES of FeS_2 is somewhat broader than that of $CuFeS_2$, although the splitting is not resolved.

Finally, XES (Cu Lα, S $L_{2,3}$ and S $K\beta_1$) and XPS VB for CuS are shown in figure 9, and should be compared with the computed DOS in figure 6. The broad feature in the S $L_{2,3}$
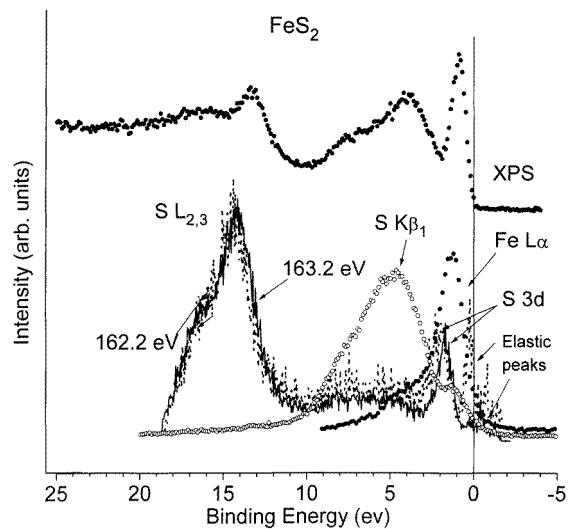
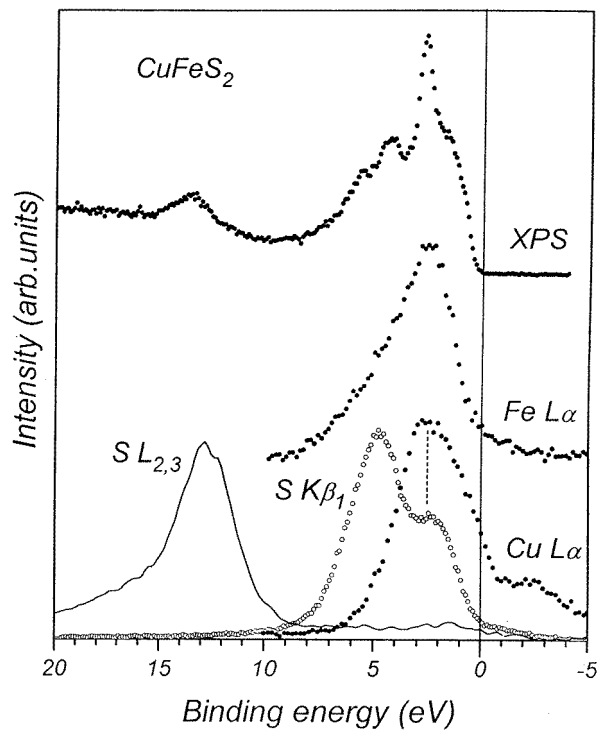**Figure 7.** Comparison of XES and XPS VB emission for FeS_2.

Figure 8. Comparison of XES and XPS VB emission for $CuFeS_2$.

XES is attributed to the S 3s band located at binding energies between 12 eV and 16 eV in figure 6. The feature in S $L_{2,3}$ XES around 3 eV binding energy corresponds to S 3d density of states. The S $K\beta_1$ XES has a main peak at a binding energy of 5 eV and a shoulder

at lower binding energy, where the S 3p band hybridizes with Cu 3d. Figure 6 indicates both the main S 3p band as well as S 3p/Cu 3d hybridization. As predicted by the LMTO calculations, CuS appears to be metallic on the basis of Cu Lα XES shown in figure 9. However, the Cu 3d band in figure 6 seems to be slightly narrower than what would be expected on the basis of the Cu Lα XES. This may be an artifact of the atomic sphere approximation, and can in principle be removed with a full-potential treatment. In spite of this minor discrepancy there is a one-to-one correspondence between the main features in figures 6 and 9.
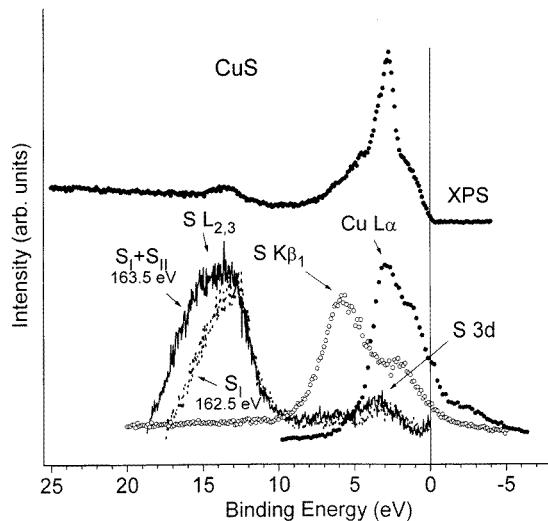

Figure 9. Comparison of XES and XPS VB emission for CuS.

The level of agreement between the experiments and the LMTO calculations is very good. Therefore it is valid to use the results of these electronic structure calculations of CuS, FeS$_2$ and CuFeS$_2$ to aid the interpretation of the excitation energy dependence of S L$_{2,3}$ XES of CuS.

4. Conclusion

Results of measurements of sulphur L$_{2,3}$ x-ray emission spectra of CuS and FeS$_2$, excited by synchrotron radiation near the sulphur 2p threshold, are presented. An excitation energy dependence of the sulphur L$_{2,3}$ XES is found only for CuS, and must be attributed to the presence of inequivalent sulphur atoms in CuS. Two thirds of the sulphur atoms form S$_2$ dimers (as in FeS$_2$) while the remaining ones are single (as in CuFeS$_2$). This conclusion is confirmed by XPS measurements and LMTO electronic structure calculations for CuS, FeS$_2$ and CuFeS$_2$. State-of-the-art electronic structure calculations provide a powerful tool in the interpretation of data obtained from a broad variety of experimental techniques. It is shown that selective excitation of x-ray emission valence spectra can be used to determine the atom-decomposed partial density of states for inequivalent sites in solids occupied by chemically identical species.

Acknowledgments

References

[1] Callcott T A, Jia J J, Zhou L, Ederer D L, Terminello L J, Carlisle J A, Perera R C C, Samant M G, Himpsel F J and Arakawa E T 1996 *Mater. Res. Soc. Symp. Proc.* vol 437 (Pittsburgh, PA: Materials Research Society) p 137
[2] Nordgren E J 1996 *J. Electron Spectrosc. Relat. Phenom.* **78** 25
[3] Krause M O 1979 *At. Nucl. Data Tables, J. Chem. Phys. Ref. Data* **8** 307
[4] Lawniczak-Jablonska K *et al* 1996 *Preprint LBNL-39756, UC-404*
[5] Kurmaev E Z *et al Mater. Trans.* submitted
[6] Kurmaev E Z *et al J. Phys.: Condens. Matter* submitted
[7] Guo J-H, Butorin S M, Wassdahl N, Skytt P, Nordgren J and Ma Y 1994 *Phys. Rev.* B **49** 1376
[8] Butorin S M, Guo J-H, Wassdahl N, Skytt P, Nordgren J, Ma Y, Ström C, Johansson L-G and Qvarford M 1995 *Phys. Rev.* B **51** 11 915
[9] Kurmaev E Z *et al Phys. Rev.* B **57** at press
[10] Jia J J *et al* 1995 *Rev. Sci. Instrum.* **66** 1394
[11] Kurmaev E Z, Fedorenko V V, Shamin S N, Postnikov A V, Wiech G and Kim Y 1992 *Phys. Scr.* T **41** 288
[12] Dolgih V E, Cherkashenko V M, Kurmaev E Z, Goganov D A, Ovchinnikov E K and Yarmoshenko Yu M 1984 *Nucl. Instrum. Methods* **224** 117
[13] Anderson O K 1975 *Phys. Rev.* B **12** 3060
[14] Kohn W and Sham L J 1965 *Phys. Rev.* A **140** 1133
[15] von Barth U and Hedin L 1972 *J. Phys. C: Solid State Phys.* **5** 1629
[16] Wyckoff R W G 1964 *Crystal Structures* (New York: Wiley)
[17] Hamajima T, Kambara T, Gondaira K I and Oguchi T 1981 *Phys. Rev.* B **24** 3349
[18] Evans H T Jr and Konnert J A 1976 *Am. Mineral.* **61** 996
[19] Fujisawa M, Suga S, Mizokawa T, Fujimori A and Sato K 1994 *Phys. Rev.* B **49** 7155
[20] Dyatkina M E and Klimenko N M 1973 *J. Struct. Chem. (USSR)* **14** 172
[21] Mazalov L N, Yumatov V D, Murahtanov V V, Gelmukhanov F Kh, Dolenko G N, Gluskin E S and Kondratenko A V 1977 *X-ray Spectra of Molecules* (Novosibirsk: Nauka)
[22] Wiech G, Feldhutter H-O and Simunek A 1993 *Phys. Rev.* B **47** 6981
[23] Galakhov V R *et al* 1995 *J. Phys.: Condens. Matter* **7** 5529
[24] Simunek A, Polcik M and Wiech G 1995 *Phys. Rev.* B **52** 11 865
[25] Yarmoshenko Yu M 1997 *J. Phys.: Condens. Matter* **9** 9403